Inelastic neutron scattering of H_2 adsorbed in HKUST-1

Y. Liu [a,b], C.M. Brown [b,c,*], D.A. Neumann [b], V.K. Peterson [d], C.J. Kepert [d]

[a] *Department of Materials and Engineering, University of Maryland, College Park, MD 20742, USA*
[b] *NIST Center for Neutron Research, 100 Bureau Drive, Gaithersburg, MD 20899-8562, USA*
[c] *Indiana University Cyclotron Facility, Indiana University, 2401 Milo B. Sampson Lane, Bloomington, IN 47408, USA*
[d] *School of Chemistry, The University of Sydney, NSW 2006, Australia*

Abstract

A series of inelastic neutron scattering (INS) investigations of hydrogen adsorbed in activated HKUST-1 ($Cu_3(1,3,5$-benzenetricarboxylate)$_2$) result in INS spectra with rich features, even at very low loading (<1.0 H_2:Cu). The distinct inelastic features in the spectra show that there are three binding sites that are progressively populated when the H_2 loading is less than 2.0 H_2:Cu, which is consistent with the result obtained from previous neutron powder diffraction experiments. The temperature dependence of the INS spectra reveals the relative binding enthalpies for H_2 at each site.
Published by Elsevier B.V.

Keywords: Energy storage materials; Hydrogen storage materials; Neutron scattering

1. Introduction

Stimulated by the interest to move to a hydrogen economy, there has been an intensive research effort in recent years to look for suitable methods and materials that can store hydrogen in accordance with the requirements designated by the U.S. Department of Energy. Many different classes of materials have been investigated such as metal hydrides, chemical hydrides and physisorbed hydrogen molecules on carbon-based materials. Currently, no material can simultaneously reach the efficiency, size, weight, cost and safety requirements for transportation usage. Amongst them, the physisorption method has the advantage of fast kinetics, good reversibility and low heat load managements upon hydrogen storing.

In order to reach high-density hydrogen storage via physisorption, high surface areas are necessary. Different materials, such as carbon nanotubes, activated carbons, carbide-derived carbons and metal organic frameworks (MOFs), have been investigated [1–7]. Among them, MOFs have high surface areas, are relatively easy to synthesize and have the flexibility of modifiable components [1,2,5,6]. It was reported that MOF-

5 ($Zn_4O(1,4$-benzenedicarboxylate)$_2$) can store up to 10 wt% hydrogen indicating that there is significant internal space available for hydrogen storage [6]. However, due to low binding energies, this saturation loading can only be realized at cryogenic temperatures. While a recent study has stated that about 15 kJ/mol would be an ideal enthalpy for H_2 adsorption at room temperature [8], the initial enthalpy of adsorption of MOF-5 [1], activated carbons and nanotubes [9] is around 5–6 kJ/mol. Therefore, it is important to find ways to improve the H_2 binding energy.

It has been shown that tuning pore sizes, and exposing metal centers can significantly improve the H_2 adsorption enthalpy at 77 K [1,10,11]. The initial enthalpy of H_2 adsorption is about 6.6 kJ/mol for HKUST-1 [1], 7.4 kJ/mol for Prussian blue analogues [7], 8.3 kJ/mol for MOF-74 ($Zn_2(C_8H_2O_6)$) [1], 8.4 kJ/mol for $Mn_3(1,4$-benzeneditetrazolate)$_3$ [12], 8.7 kJ/mol for $Zn_3(1,4$-benzeneditetrazolate)$_3$ [12], 9.1 kJ/mol for IRMOF-11 ($Zn_4O(4,5,9,10$-tetrahydropyrene-2,7-dicarboxylate)) [1], 10.1 kJ/mol for $Mn_3((Mn_4Cl)_3BTT_8)_2$ and $H_2[Co_4O(4,4',4''$-s-triazine-2,4,6-triyltribenzoate)$_{8/3}]$ [5,11]. Neutron diffraction results indicated that the primary interaction of H_2 with Prussian blue analogues occurs in its relatively smaller pores [13].

It has long been postulated that the exposed metal centers are responsible for increased H_2 adsorption enthalpies of a series of MOFs [1]. However, only recently can experimental results

---

directly attest to this effect. The direct binding between H_2 and Mn^{2+} has been observed in $Mn_3((Mn_4Cl)_3BTT_8)_2$ using neutron powder diffraction [5].

H_2 interaction with the exposed Cu atoms in HKUST-1 was previously inferred from the IR spectra of H_2 in HKUST-1 at 15 K with the assignment of the peak at approximately $4100\,cm^{-1}$ to the formation of a Cu(II)-dihydrogen complex [10]. Recently, we have identified six different D_2 adsorption sites in HKUST-1 up to a hydrogen adsorption of about 4 wt%, where the first adsorption site exhibits direct binding between D_2 and Cu(II). The distance between D_2 and Cu(II) is around 2.4 Å [14], significantly shorter than the typical 3 Å distance between physisorbed H_2/D_2 and absorbents. However, this distance is much larger than the distance of the well-known "Kubas" type binding, which ranges from 1.7 Å to 2.0 Å [15]. We note that this H_2–Cu binding distance is larger than that of H_2–Mn at 2.2 Å in $Mn_3((Mn_4Cl)_3BTT_8)_2$ [5]. The shorter interaction distance of the H_2 and Mn indicates a stronger hydrogen molecule binding, consistent with the larger initial enthalpy of H_2 adsorption observed in $Mn_3((Mn_4Cl)_3BTT_8)_2$.

From the point-of-view of bond length, this interaction between molecular hydrogen and the metal atoms is weaker than "Kubas" binding, and yet stronger than a simple Van der Waals attraction. Therefore, it is interesting to understand its properties and possible link with "Kubas" binding. Inelastic neutron scattering (INS) has been used to study the "Kubas" binding in different materials [16] and we apply it here to study the dynamics of H_2 in HKUST-1. The features of the INS spectra, associated with different H_2 adsorption sites, are discussed along with the temperature dependence of the INS spectra.

2. Experimental details

HKUST-1 is composed of 1,3,5 benzenetricarboxylate (BTC) ligands coordinating copper ions in a cubic lattice (*Fm-3m*). First reported in 1999 [17], HKUST-1 has more recently been activated for gas adsorption by desorbing the coordinated water molecules [10,14]. Sample preparation is described elsewhere [14,17]. After synthesis, the sample was desolvated by heating under vacuum to 453 K for 48 h.

Immediately before the INS experiments, the sample was further degassed at 393 K under dynamic vacuum for about 24 h. The sample (2.752 g) was transferred to a cylindrical aluminum cell equipped with a capillary gas line and a packless valve, and sealed with an indium o-ring. The sample was mounted onto a sample stick, equipped with a stainless-steel gas line with an additional valve for a use in closed-cycle helium refrigerator. All sample transfers were performed in a helium-filled glove box equipped with water and oxygen monitors.

The INS spectra were collected using the Filter Analyzer Neutron Spectrometer (FANS) at the National Institute of Standards and Technology Center for Neutron Research (NCNR) [18]. We used a pyrolytic graphite monochromator bracketed between two Söller collimators (of 20′ and 20′ divergence before and after the monochromator, respectively) to produce a collimated, monoenergetic beam of neutrons, which was directed onto the sample. The energy transferred to the sample was determined by passing the scattered neutrons through a low-energy, band-pass filter consisting of polycrystalline Bi, Be, graphite, and then Be again before reaching the ^{3}He detectors. For the filter arrangement used in this study, the cut-off energy was about 1.8 meV with an energy resolution of 1.1 meV. The primary spectrometer contributes slightly to the resolution in the region around 15 meV so that the overall energy resolution is 1.2 meV.

The INS spectrum of the bare material (0 H_2:Cu) was first measured at approximately 4 K and used as the background. Subsequently, H_2 quantities corresponding to selected H_2:Cu ratios between 0.1 and 4.0 were loaded into the sample from a known volume. During each H_2 dosing the sample was first heated

to above 70 K and the H_2 gas was allowed to reach equilibrium. The sample was then slowly cooled and the INS spectrum measured at approximately 4 K. In all cases, the system pressure reading was zero well before reaching 25 K.

3. Results and discussion

Neutron diffraction experiments reveal three distinct H_2 adsorption sites up to a loading of 2.0 H_2:Cu ($\sim$2 wt%) [14]. The crystal structure and adsorption sites are depicted in Fig. 1 and labeled I, II, and III. Following binding at the Cu^{2+} sites (site I), hydrogen molecules are absorbed into the small octahedral cage (site II). However, due to the small space available in this cage, the equivalent of only one hydrogen molecule is adsorbed at low loadings. Site III is located at the window of four, tetrahedrally arranged, open faces of the octahedral cage. At larger H_2:Cu loadings, it is possible to put more hydrogen molecules into the small cage at a different symmetry site [14].

A hydrogen molecule is composed of two indistinguishable fermions and can be considered a good quantum rotor. As such, the total wavefunction must be antisymmetric upon exchange of the nuclei. A hydrogen molecule is in the *para* state when the total nuclear spin, S, is zero and the associated quantum rotation number, J, is even. In the *ortho* state $S = 1$ and the associated J is odd. In general, neutrons can interact with the hydrogen molecule, causing a nuclear spin-flip, and convert it between the *para* and *ortho* states [19–21]. This process is proportional to the incoherent cross section, which is about 46 times larger than coherent scattering between *para* only states [21]. With the assumption that the majority of hydrogen molecules are in the *para* state, the INS spectra are dominated by *para-ortho* transitions or dynamics coupled with the *para–ortho* transition [21]. Since, incoherent scattering only reflects the dynamics of individual particles, it is therefore possible to subtract a background spectrum from the spectrum of interest to obtain the INS spectrum of the dosed H_2 [22].

Fig. 2 shows the INS spectra at 0.2, 0.5, 1.0, 1.5, and 2.0 H_2:Cu loadings from which the spectrum at 0 H_2:Cu has been subtracted. At 0.2 and 0.5 H_2:Cu only site I is populated. The INS spectra are then attributable to the dynamics of H_2 molecules directly binding to Cu^{2+} ions. Therefore, we can assign peak 1 to H_2 dynamics at site I. According to the neutron diffraction study
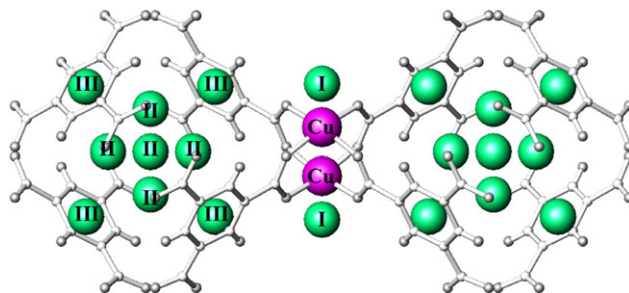

Fig. 1. First three H_2 adsorption sites in HKUST-1 labeled I, II, and III. Green (gray) balls illustrate the positions of the different hydrogen sites while the pink (dark gray) balls are Cu^{2+} ions. All other atoms and bonds are shown in pale gray (not to scale). (For interpretation of the references to colour in this figure legend, the reader is referred to the web version of the article.)
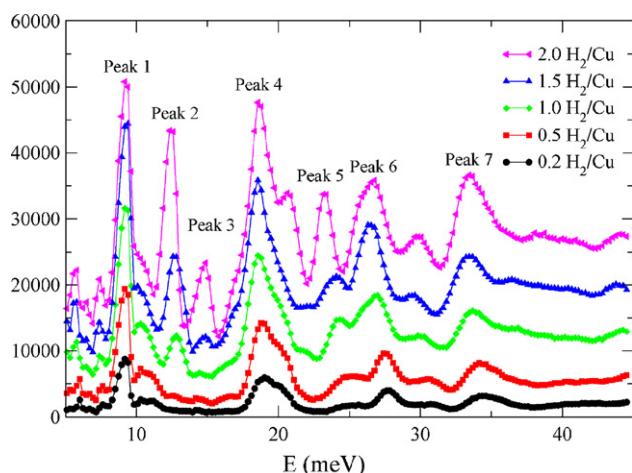
Fig. 2. INS spectra of H_2 in HKUST-1 at 0.2, 0.5, 1.0, 1.5, 2.0 H_2:Cu. The background spectrum has been subtracted from the H_2 spectra.

Fig. 3. The area of peaks 1, 2, and 3 as a function of H_2 loadings.

[14], hydrogen molecules should next populate site II, giving rise to peak 2, and likely peak 5 due to the parallel increase in intensity with peak 2. We attribute peak 3 to hydrogen dynamics at site III. Peaks 4, 6, and 7 are primarily due to site I at low loadings and become more complicated when the H_2 loading increases. Better energy resolution is needed in order to resolve the possible features contained in these peaks and clearly distinguish rotational sublevels and peaks of possible rotation-vibration origin. Therefore, we will focus our discussion on peaks 1, 2, and 3 which we assign to sites I, II, and III respectively.

At the different loadings, the position of peaks 1 and 3 do not shift significantly while the position of peak 2 does. This change could be explained by the fact that when H_2 is progressively loaded to site III, the overall potential the H_2 experiences inside the small cage changes. This explanation is consistent with the observation from additional data (not shown) that the shift of peak 2 is concomitant with the increase in intensity of peak 3.

For a free hydrogen molecule, the *para–ortho* transition is associated with a $J = 0$ to $J = 1$ excitation, whose excitation energy is 14.7 meV. Due to the local potential at the adsorption site, $J = 1$ can further split into three sublevels, which cause the rotation transition peak to split into two or three peaks. The energy difference between the split peaks can be small, on the order of 1.7 meV for H_2 in carbon materials [23,24], or large as 25 meV for H_2 in partially cobalt exchanged type A zeolite [16]. The breadths of peaks 1, 2, and 3 are resolution limited with the full-width at half maximum (FWHM) of about 1.2 meV. Therefore, if there are multiplets contained within these peaks, the splitting must be much less than the FWHM. There is a small broad peak next to peak 1, which might arise due to either the splitting of $J = 1$, or a rotation–translation coupling, or translational motions of *ortho* H_2 that are not converted to *para* H_2 via intereaction with the host material [24]. The energy positions of peaks 1 and 3 are at 9.2 meV and 14.8 meV, respectively, while the position of peak 2 shifts from 12.9 meV at 1.0 H_2:Cu to 12.4 meV at 2.0 H_2:Cu. The significant downshift of peaks 1 and 2 from the free rotor value contains information of the interaction between H_2 and host matrix, which will be addressed in a future paper.
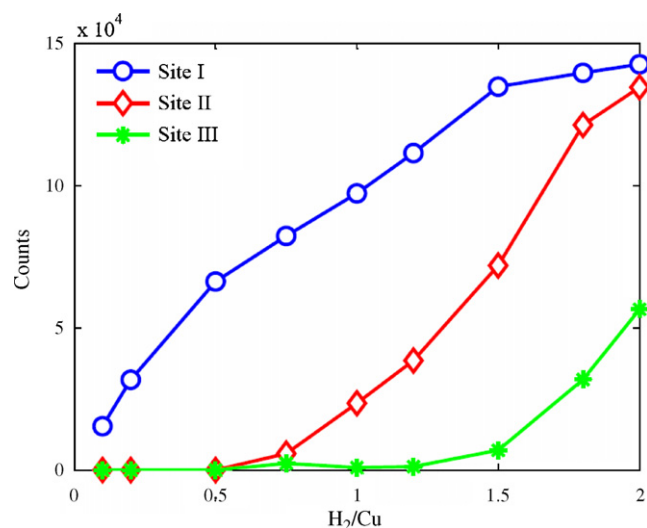
Fig. 3 shows the areas of peaks 1, 2, and 3 as a function of hydrogen loadings. Although, it is not meaningful to compare the areas of the different peaks, the growth of each peak should qualitatively agree with the amount of absorbed H_2 at the corresponding site. If we assume that at 2 H_2:Cu, both sites I and II are fully populated as shown by diffraction, site I is saturated first at around 1.5 H_2:Cu, while site II begins to be populated after 0.5 H_2:Cu and is fully populated at around 1.8 H_2:Cu. Site III begins to adsorb H_2 only after about 1.5 H_2:Cu and continues to be populated up to and possibly beyond 2.0 H_2:Cu. These observations are consistent with the recent neutron diffraction results although the INS results may not be as accurate as site occupancy determined through diffraction measurements.

To estimate the binding strength of different sites, we performed temperature dependent INS experiments. Having first measured the sample with 4 H_2:Cu at 4 K, we then raised the temperature to T_h, where the sample was degassed for over 30 min until the dynamic pressure was less than 40 Pa. After cooling the sample back to 4 K, we measured the INS spectrum of the remaining H_2 inside the sample. By varying T_h from low to high temperatures, we then have a series of spectra representing the bound hydrogens. Extracting the areas of peaks 1, 2, and 3 allowed an estimation of enthalpy of H_2 desorption at different sites. We raised T_h sequentially to 44.2 K, 49.4 K, 58.8 K, 63.7 K, and 71.5 K. Fig. 4 shows the areas of peaks 1, 2, and 3 as a function of the degassing temperature. As expected, the binding strength of site I is greater than that observed in single-walled carbon nanotubes (SWNT) since there is still significant hydrogen left in the sample even after pumping at $T_h = 71.5$ K, while almost all physisorbed H_2 in SWNTs can be degassed out at around 65 K [19]. Therefore, the adsorption enthalpy at site I could be between 6 kJ/mol and 10 kJ/mol. As for site II, there is significant hydrogen remaining at about 60 K. Therefore, we speculate that the adsorption enthalpy is comparable to the initial H_2 adsorption enthalpy in some SWNT, which is around 5–6 kJ/mol as shown by computer simulations [9]. The adsorption enthalpy of site III is much smaller than that of sites I and II because most hydrogen molecules are degassed out at
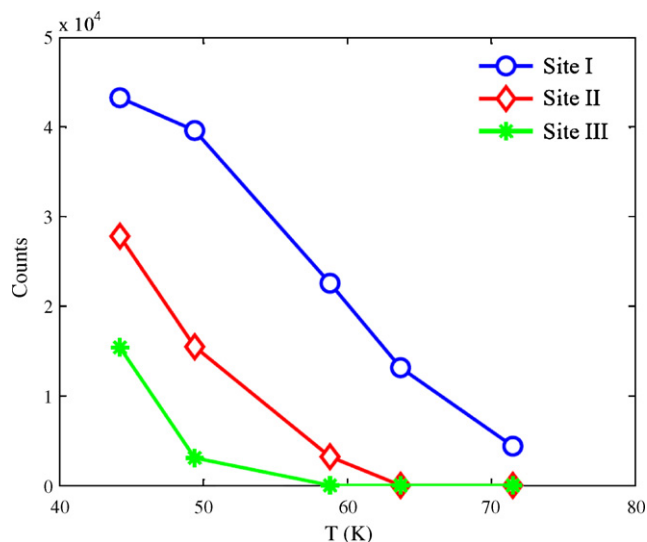
Fig. 4. The area of peaks 1, 2, and 3 as a function of degassing temperature, T_h.

55 K. Therefore, it is reasonable that the adsorption enthalpy for site III is less than 5 kJ/mol. The above estimation is very coarse for the reasons that follow. Experiments on H_2 in SWNT [19] were performed under isosteric conditions while we degassed the sample and then obtained the spectra after cooling the sample down to approximately 4 K. The advantage of our experiment is that the measurement is self-consistent since the Debye–Waller factor no longer varies with temperature. Additionally, at the degassing temperature, several binding sites may lose hydrogen simultaneously. When the sample cools, the hydrogen molecules in weaker binding sites may redistribute to stronger adsorption sites, which needs to be taken into consideration. Nevertheless, this method provides a simple way to study the relative binding strength of H_2 absorbed in microporous crystalline samples and compare the binding energies of the different sites.

4. Conclusions

We have measured the INS spectra of H_2 absorbed in HKUST-1. By analyzing the characteristic features observed in the INS spectra, the behavior of H_2 in HKUST-1 as a function of loading is measured. We observe three distinct spectral features that correspond to the first three binding sites. The interpretation is consistent with the results obtained from neutron powder diffraction experiments. The relative H_2 adsorption enthalpy is estimated based on temperature dependent experiments and from comparing to H_2 in SWNTs.

References

[1] J.L.C. Rowsell, O.M. Yaghi, J. Am. Chem. Soc. 128 (2006) 1304–1315.
[2] N.L. Rosi, J. Eckert, M. Eddaoudi, D.T. Vodak, J. Kim, M. O'Keeffe, O.M. Yaghi, Science 16 (2003) 1127.
[3] A.C. Dillion, K.M. Jones, T.A. Bekkedahl, C.H. Kiang, D.S. Bethune, M.J. Heben, Nature (London) 386 (1997) 377.
[4] (a) R. Chahine, T.K. Bose, Int. J. Hydrogen Energy 19 (1994) 161;
(b) Y. Gogotsi, R.K. Dash, G. Yushin, T. Yildirim, G. Laudisio, J.E. Fischer, J. Am. Chem. Soc. 127 (2005) 16006.
[5] M. Dinca, A. Daily, Y. Liu, C.M. Brown, D.A. Neumann, J. Long, J. Am. Chem. Soc. 128 (2006) 16876.
[6] T. Yildirim, M.R. Hartman, Phys. Rev. Lett. 95 (2005) 215504.
[7] S.S. Kaye, J.R. Long, J. Am. Chem. Soc. 127 (2005) 6506.
[8] S.K. Bhatia, A.L. Myers, Langmuir 22 (2006) 1688.
[9] (a) J. Li, T. Furuta, H. Goto, T. Ohashi, Y. Fujiwara, S. Yip, J. Chem. Phys. 119 (2003) 2376;
(b) P. Benard, R. Chahine, Langmuir 17 (2001) 1950.
[10] C. Prestipino, L. Regli, J.G. Vitillo, F. Bonino, A. Damin, C. Lamberti, A. Zecchina, P.L. Solari, K.O. Kongshaug, S. Bordiga, Chem. Mater. 18 (2006) 1337.
[11] S. Ma, H.C. Zhou, J. Am. Chem. Soc. 128 (2006) 11734.
[12] M. Dinca, A.F. Yu, J.R. Long, J. Am. Chem. Soc. 128 (2006) 8904.
[13] M.R. Hartman, V.K. Peterson, Y. Liu, S.S. Kaye, J.R. Long, Chem. Mater. 18 (2006) 3321.
[14] V.K. Peterson, Y. Liu, C.M. Brown, C.J. Kepert, J. Am. Chem. Soc. 128 (2006) 15578.
[15] (a) G.J. Kubas, Acc. Chem. Res. 21 (1988) 120;
(b) G.J. Kubas, Organomet. Chem. 635 (2001) 37.
[16] J.M. Nicol, J. Eckert, J. Howard, J. Phys. Chem. 92 (1988) 7117.
[17] S.S.-Y. Chui, S.M.-F. Lo, J.P.H. Charmant, A.G. Orpen, I.D. Williams, Science 283 (1999) 1148.
[18] T.J. Udovic, D.A. Neumann, J. Leao, C.M. Brown, Nucl. Instrum. Methods A517 (2004) 189.
[19] C.M. Brown, T. Yildirim, D.A. Neumann, M.J. Heben, T. Gennet, A.C. Dillon, J.L. Alleman, J.E. Fischer, Chem. Phys. Lett. 329 (2000) 311.
[20] D.G. Narehood, M.K. Kostov, P.C. Eklund, M.W. Cole, P.E. Sokol, Phys. Rev. B 65 (2002) 233401.
[21] J.A. Young, J.U. Koppel, Phys. Rev. A 135 (1964) 603.
[22] S.H. Chen, M. Kotlarchyk, Interaction of Photons and Neutrons with Matters, World Scientific, Singapore, 1997.
[23] P.A. Georgiev, D.K. Ross, A. De Monte, U. Montaretto-Marullo, R.A.H. Edwards, A.J. Ramirez-Cuesta, D. Colognesi, J. Phys.: Condens. Matter. 16 (2004) L73.
[24] S.A. FitzGerald, T. Yildirim, L.J. Santodonato, D.A. Neumann, J.R.D. Copley, J.J. Rush, F. Trouw, Phys. Rev. B 60 (1999) 6439.